Supporting Information

An ultra-sensitive label free electrochemiluminescence CKMB immunosensor using novel nanocomposite modified printed electrode

Juthi Adhikari[a], Natasha Ann Keasberry[a], Abdul Hanif Mahadi[b], Hiroyuki Yoshikawa[c], Eiichi Tamiya[c], Minhaz Uddin Ahmed*[a]

[a] *Biosensors and Biotechnology Laboratory, Chemical Science Programme, Faculty of Science, Universiti Brunei Darussalam. Jalan Tungku Link, Gadong, BE 1410, Brunei Darussalam*

[b] *Centre for Advanced Material and Energy Sciences, Universiti Brunei Darussalam, Tungku Link, Gadong, BE1410, Brunei Darussalam*

[c] *Nanobioengineering Laboratory, Department of Applied Physics, Graduate School of Engineering, Osaka University, 2-1 Yamada-oka, Suita, Osaka 565-0871, Japan*

*Corresponding Author: minhaz.ahmed@ubd.edu.bn

S1. Reagents

Mouse monoclonal antibody CKMB and human serum Creatine Kinase-muscle brain protein (CK-MB) was procured from Shanghai Linc-Bio Science Co. LTD (Shanghai, China). Carcinoembryonic antigen (CEA), haptoglobin (HP), leptin, cortisol, human chorionic gonadotropin (hCG), C- reactive protein (CRP), alpha fetoprotein (AFP), β-2 microglobulin (β-2M), Cardiac troponin T (cTnT), Cardiac troponin I (cTnI) bovine serum albumin (BSA), sodium azide (NaN_3), potassium chloride (KCL), potassium ferrocyanide, potassium ferricyanide, Tris(2,2′-bipyridyl) dichlororuthenium(II) hexahydrate ($[Ru(bpy)_3]Cl_2.6H_2O$), tripropylamine (98% purity), Tris, disodium phosphate (Na_2HPO_4), and monosodium phosphate ($NaH_2PO_4.H_2O$) were purchased from Sigma-Aldrich (Saint Louis, USA). Chitosan (85% deacetylated) was purchased from Alfa Aesar (Ward Hill, M.A). Carbon nano-onions was purchased from Carbon Allotropes (Kensington, Australia). Colloidal solutions of gold nanoparticles (40 nm) were purchased from BBI Solutions (Cardiff, UK). Iron oxide (Fe_3O_4) was purchased from US Research Nanomaterials, Inc. (Houston, TX, USA). For all experiments, samples were diluted in 10 mM PBS at pH 7.4. All buffer, ECL probe and redox probe solutions were prepared in-house. PBS-buffer was used for preparation of redox couple $(Fe(CN)_6]^{3-}$/$[Fe(CN)6]^{4-}$) for electrochemical analysis. All chemicals and reagents were of ≥ 95% purity and used as received. All solutions were prepared using freshly obtained Milli-Q water (deionized with specific resistance ~18 $M.cm^{-1}$). Every analysis was performed at least three times (n=3) and average was represented with standard deviation. Throughout the experiment, the room temperature (RT) was 21.5 ± 0.5°C.

S2. Apparatus

For ECL measurement an MPI-A Capillary Electrophoresis Electrochemiluminescence Analyzer system was purchased from Xi′an Yima Opto-Electrical Technology Co., Ltd. (Xian, Shaanxi, Mainland China). An in-house working ECL cell was used to receive the light emitted from the ECL reactions and to conduct it to an ultra-sensitive single photon-counting module or photomultiplier tube (PMT) connected to MPI-A software. Fabricated immunosensor containing $[Ru(bpy)_3]Cl_2$-TPrA was immersed in the ECL cell (diameter 1.5 cm and height 5 cm) and mounted over PMT to receive the ECL intensity signal. To study the electrochemical layer-by-layer fabrication, kinetic study and charge analysis of the immunosensor, cyclic voltammetry (CV) and chronocoulometry (CC) techniques were

performed using an Autolab PGSTAT101 III potentiostat/galvanostat (Metrohm, Netherlands) in combination with the Autolab Nova 1.10 software. The disposable working ceramic SWCNTs- modified SPEs were obtained from DropSens (Asturias, Spain). Each of these comprise of a carbon counter electrode, a silver reference electrode, and a 4 mm diameter working electrode, with a maximum working volume of 50 µL. They are of dimensions L33 × W10 × H0.5 mm. To study the surface morphology of the nanocomposite, field-emission electron microscopy (FE-SEM) JEOL, JSM-7610F (Tokyo, Japan) was used and before each FE-SEM analysis, samples were carbon coated for 60 sec to analyze at 40, 000× magnification, having SEI mode at 5. 0 kV with 100 nm scale. And for TEM analysis, Transmission electron microscope (Japan), HF-2000 (Hitachi) was being used at an acceleration voltage of 200 kV. The X-ray Diffraction (XRD) measurements were performed with Shimadzu XRD-700 Maxima X-ray Diffractometer. All analyses were performed at room temperature and atmospheric pressure (21±1 °C, air-conditioned laboratory). All experimental points are an average of three replicates obtained with three different fabricated immunosensors.

S3. Optimization of anti-CKMB concentration and anti-CKMB immobilization time:

During the fabrication of the CKMB immunosensor, several parameters were optimized. These included: (i) anti-CKMB concentration, (ii) anti-CKMB immobilization on the CNOs/Fe_3O_4/AuNPs/CS/SWCNTs-SPE platform at 21.5 ± 0.5°C. The working concentration for anti-IgA was selected by spiking different concentrations of CKMB antibody (1 µg mL^{-1}, 10 µg mL^{-1} and 20 µg mL^{-1}) on the BSA/CNOs/Fe_3O_4/AuNPs/CS/SWCNTs-SPE immunosensor in the presence of 100 pg mL^{-1} CKMB and subsequently, 10µg mL^{-1} was selected as antibody working concentration. Blocking was carried out for 1 hr and antibody and antigen incubation time was 60 min at 21.5 ± 0.5 °C (Supplementary Fig. S1 (A)). Next, the optimum incubation time for CKMB antibody was determined by testing four-time frames (4 hours, 6 hours, 12 hours and overnight (14 ± 1 hrs)) and measuring the CV response accordingly. Maximum response was recorded at overnight (14 ± 1 hrs) incubation (Supplementary Fig. S1 (B)) and hence was selected as optimal incubation time. Blocking time by BSA was chosen as 60 min and antigen-antibody reaction was carried out for 60 min at 21.5 ± 0.5°C in 10 mM PBS, pH 7.4 (n=3) for further analysis.

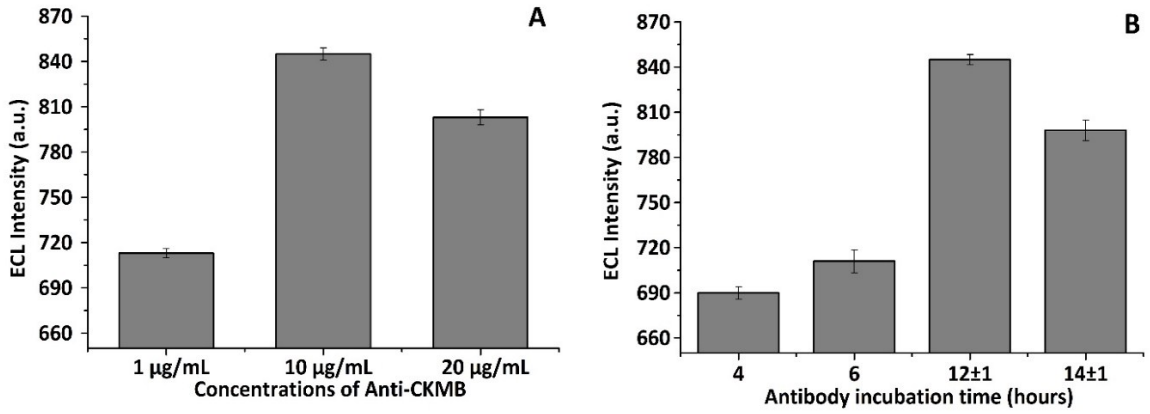

Fig. S1 (A) Different concentrations of anti-CKMB (1 µg mL^{-1}, 10 µg mL^{-1}, and 20 µg mL^{-1}) were spiked on the BSA/anti-CKMB/CS/Fe_3O_4/AuNPs/CNOs/SWCNTs immunosensor in the presence of 100 pg mL^{-1} CKMB based on the ECL intensity using CV. Blocking was carried out for 1 hr and antibody and antigen incubation time was 60 minutes. **(B)** Optimization of anti-CKMB (10µg mL^{-1}) incubation time on BSA/anti-CKMB/CS/Fe_3O_4/AuNPs/CNOs/SWCNTs platform in the presence of 100 pg mL^{-1} CKMB based on the ECL intensity using CV. Blocking time was chosen as 1 hour and immune-complex formation was carried out for 60 min at 21.5 ± 0.5°C in 10 mM PBS, pH 7.4 (n=3).

S4. Optimization of blocking by BSA, Antibody-Antigen reaction time:

Following all the optimizations mentioned above, two more crucial parameters were also optimized to ensure maximum sensitivity of the proposed immunosensor: (i) blocking time by BSA and (ii) Immunocomplex formation time. For blocking by 1% BSA in 0.1% NaN_3 prepared in 10 mM PBS, pH 7.4; 30, 60 and 90 min incubation times were tested to minimize nonspecific binding at the surface of anti-CKMB/ CNOs/Fe_3O_4/AuNPs/CS/SWCNTs-SPE-CKMB immunosensor. Maximum CV peak was found at 60 min (Supplementary Fig. S2 (A)), therefore, 60 min was used as the standard blocking time. To obtain the optimum immunoreaction time for the formation of immunocomplex between anti-CKMB and CKMB (100 pg mL^{-1}) 30, 60 and 90 min were tested on the fabricated BSA/anti-CKMB/CNOs/Fe_3O_4/AuNPs/CS/SWCNTs-SPE-CKMB immunosensors. Immunosensor response was maximum for the 60 min incubation (Supplementary Fig. S2 (B)), hence 60 min was selected as the optimum time for immunocomplex formation time between anti-CKMB and CKMB at 21.5 ± 0.5°C in 10 mM PBS, pH 7.4 (n=3) for various analytical performances of the immunosensor.

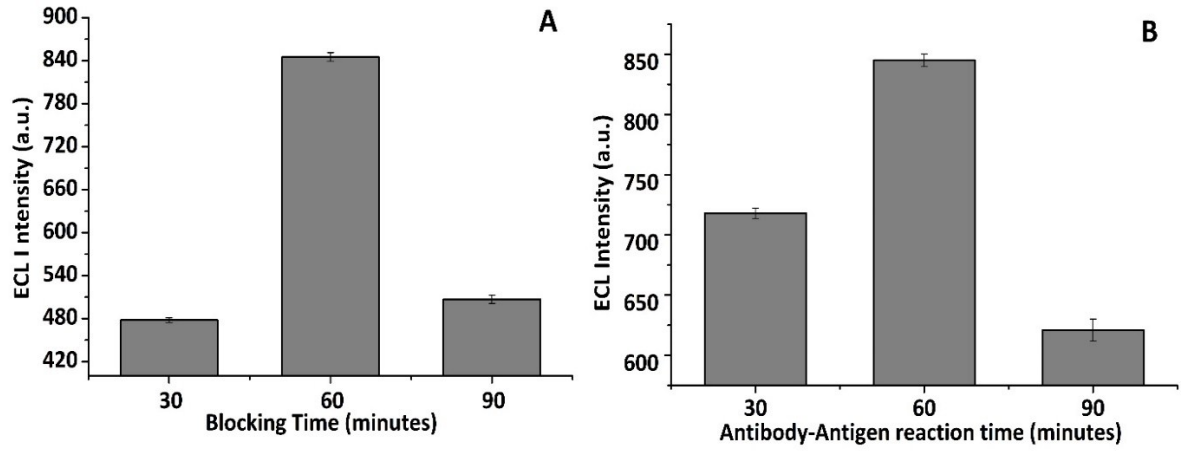

Fig. S2 (A) ECL Graph of blocking time by 0.1% BSA in 0.1% NaN_3 prepared in 10 mM PBS, pH 7.4 spiked on anti-CKMB/CS/Fe_3O_4/AuNPs/CNOs/SWCNTs for 30, 60 and 90 min based on the ECL intensity using CV. Anti-CKMB was incubated for overnight (14 ± 1) hrs and immunocomplex formation was carried out for 60 min at 21.5 ± 0.5°C. CV analysis was performed in the presence of 1:100 $[Ru(bpy)_3]Cl_2$-TPrA solution in 10 mM PBS, pH 7.4 (n = 3) at 21.5 ± 0.5°C. **(B)** Immunocomplex formation were carried out for 30, 60 and 90 min with 100 pg mL^{-1} IgA on BSA/anti-IgA/EDC-NHS/GNPs/GCE immunosensors with anti-IgA incubated for 2 h and blocked for 60 min at 21.5 ± 0.5° C.CV analysis was performed in the presence of $[Ru(bpy)_3]Cl_2$-TPrA mediator containing 10 mM PBS, pH 7.4 (n = 3).

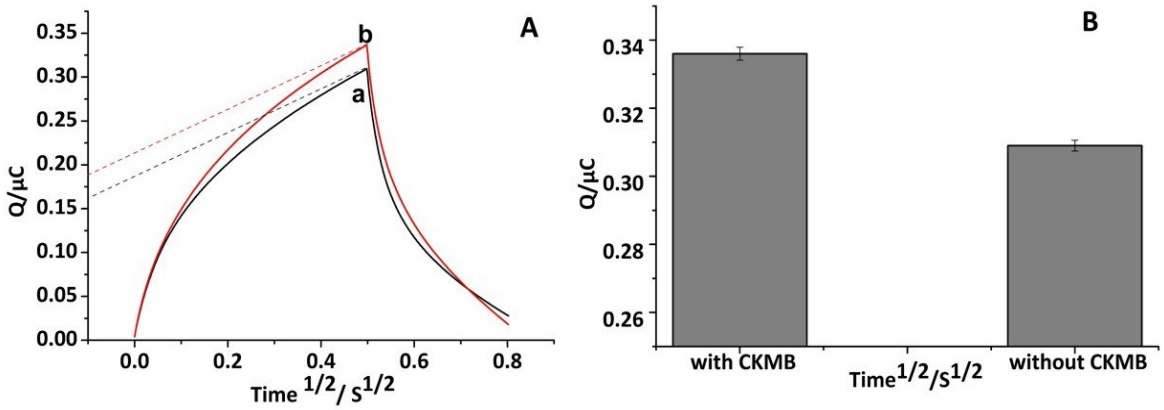

Fig. S3 Chronocoulometry analysis to confirm for $[Ru(bpy)_3]Cl_2$-TPrA diffusion-controlled electrochemical process. **(A)**: Chronocoulometry curve without CKMB (a); and with 100 pg/mL CKMB (b). **(B)**: bar diagram with CKMB (100 pg/mL) and without CKMB. Error bars indicate the standard deviations of at least three replicates (n = 3).

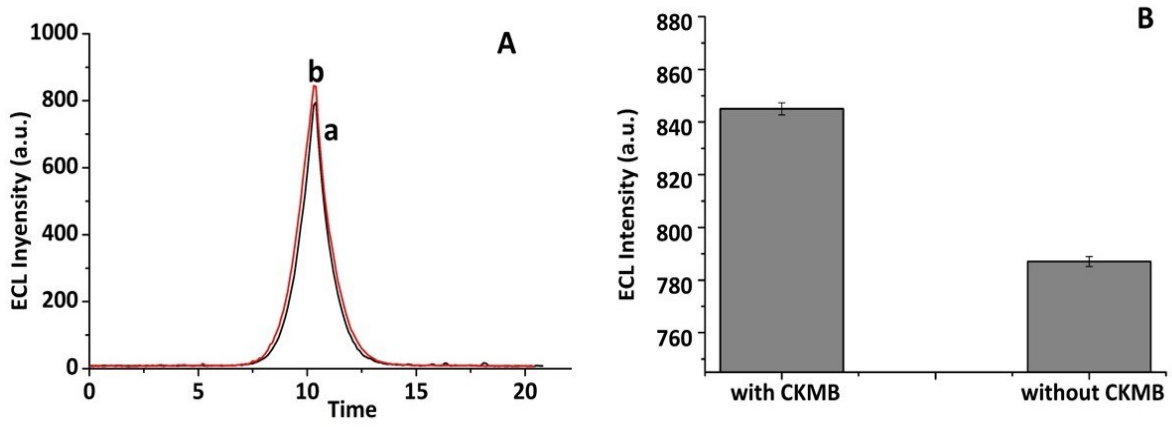

Fig. S4 Analysis of the analytical performance of the immunosensor in detecting CKMB. **(A)** Line graph of ECL intensity of the fabricated CKMB immunosensor (SWCNTs-SPE /CNOs/ Fe_3O_4/ AuNPs -CS/anti-CKMB/BSA) (a) without CKMB and (b) with CKMB. **(B)** Bar graph of the ECL signal recorded on the sensor with 100 pg/mL CKMB and without CKMB.

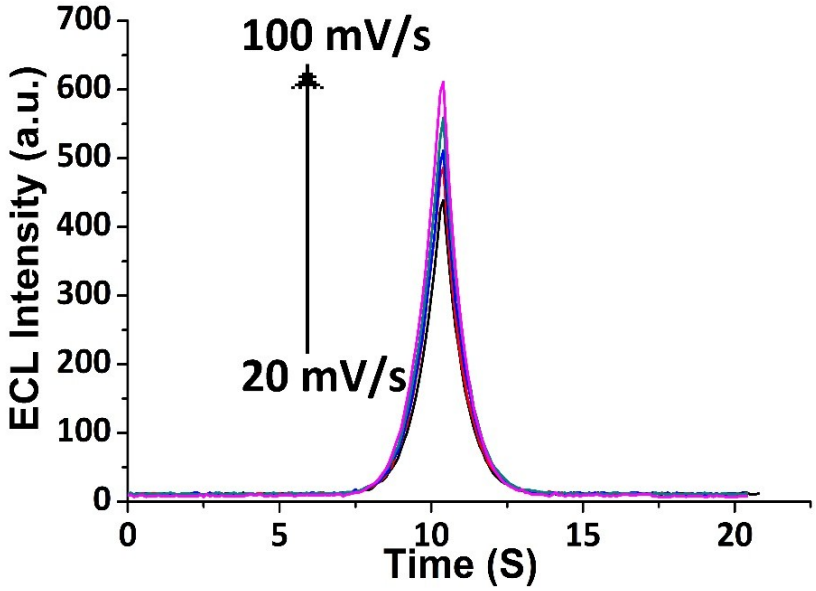

Fig. S5 Diffusion kinetic analysis as assessed by ECL intensity: ECL intensity of the fabricated immunosensor from 20 mV/s to 100 mV/s scan rate at an interval of 20, applying cyclic voltammograms of CKMB iimunosensors (from inner to outer cycle) by using 1:100 $[Ru(bpy)_3]Cl_2$-TPrA solution containing 10 mM PBS, pH 7.4 at 21.5 ± 0.5°C (n=3).

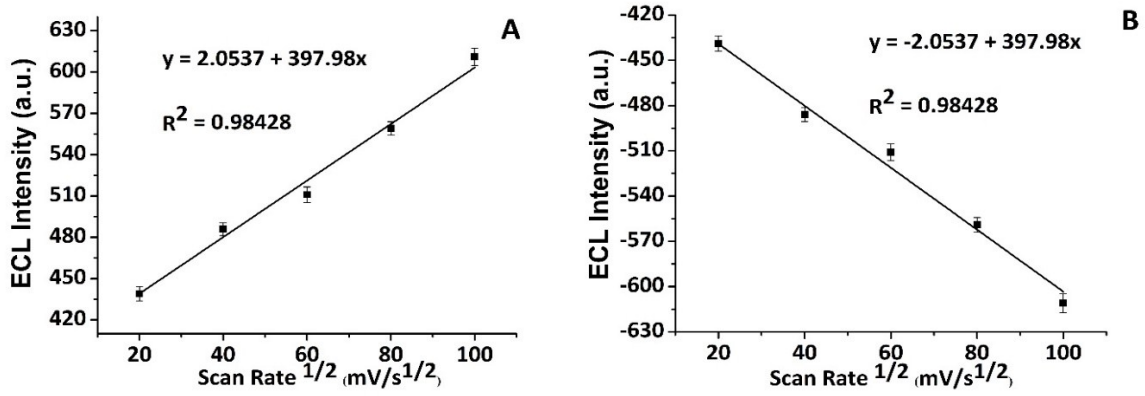

Fig. S6 Diffusion kinetic analysis as assessed by ECL intensity: **(A)** Dependence of oxidation peak currents on the square root of the scan rates and **(B)** Dependence of reduction peak currents on the square root of the scan rates using 1:100 $[Ru(bpy)_3]Cl_2$-TPrA solution containing 10 mM PBS, pH 7.4 at 21.5 ± 0.5°C (n=3).

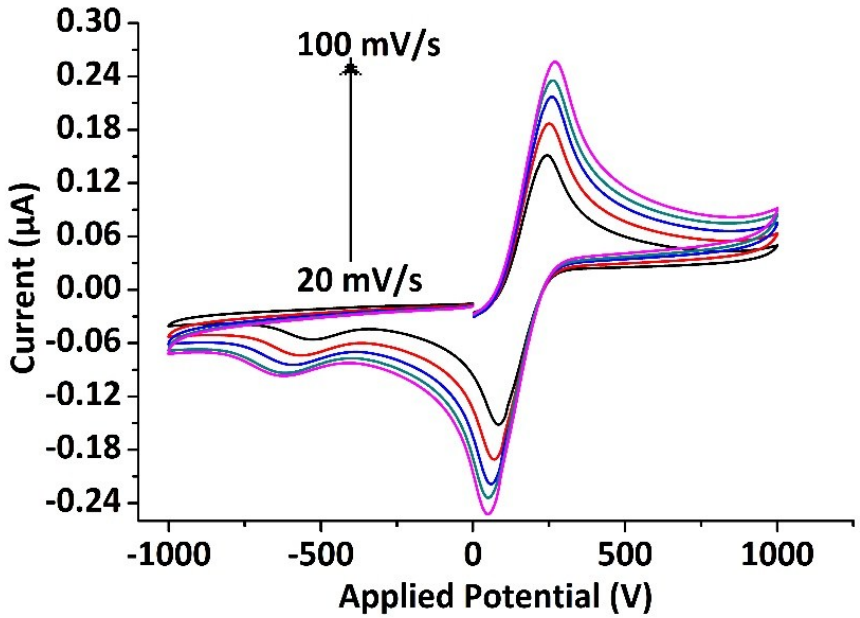

Fig. S7 Diffusion kinetic analysis as assessed by EC: Cyclic voltammograms of CKMB immunosensor from 20 mV/s to 100 mV/s (from inner to outer cycle) by using 5mM $[Fe(CN)_6]^{3-}$/ $[Fe(CN)_6]^{4-}$ redox probe containing 0.1 M KCl in solution of 10 mM PBS, pH 7.4 at 21.5 ± 0.5°C (n=3).

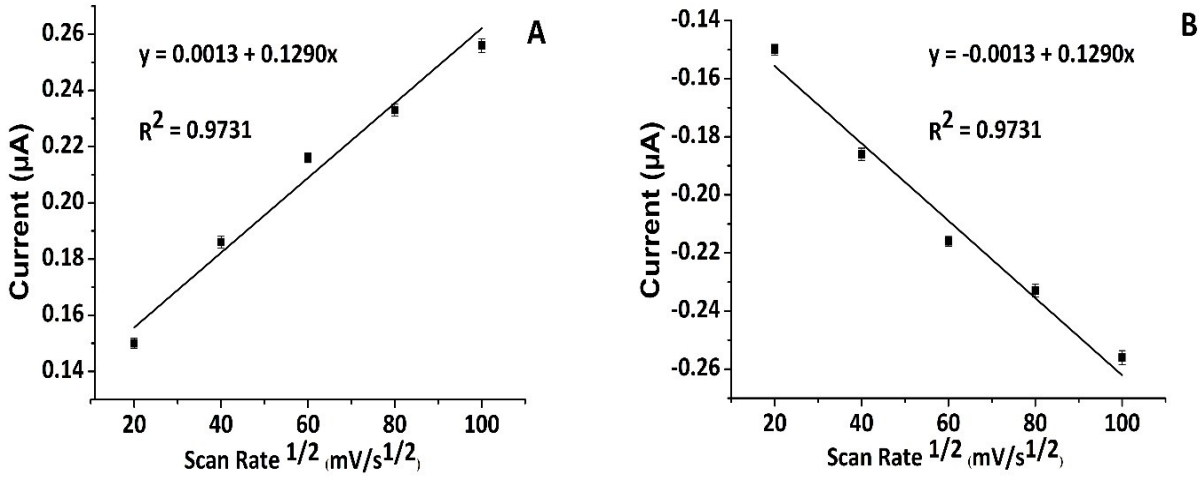

Fig. S8 Diffusion kinetic analysis as assessed by EC: **(A)** Dependence of oxidation peak currents on the square root of the scan rates and **(B)** Dependence of reduction peak currents on the square root of the scan rates using 5mM $[Fe(CN)_6]^{3-}$/ $[Fe(CN)_6]^{4-}$ redox probe containing 0.1 M KCl in solution of 10 mM PBS, pH 7.4 at 21.5 ± 0.5°C (n=3).

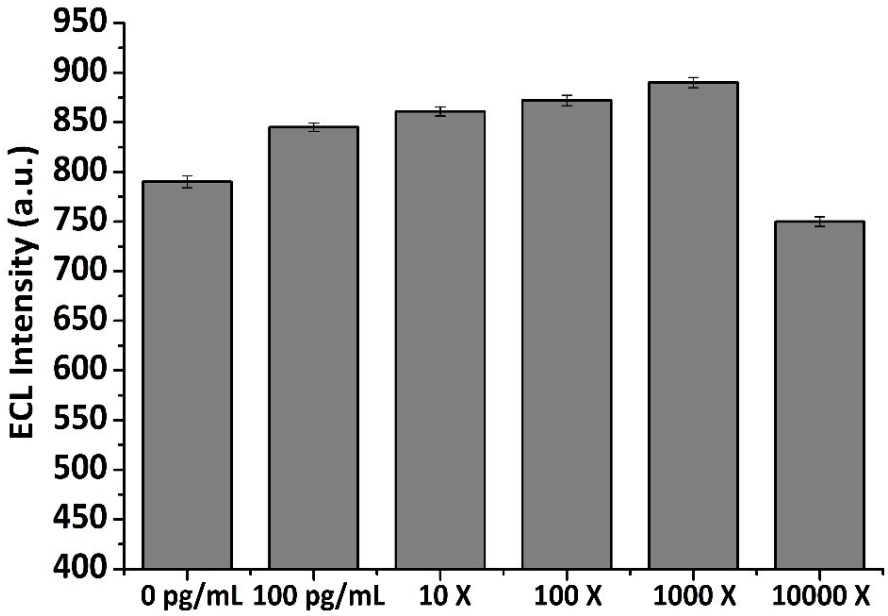

Fig. S9 Optimization of the dilution factor of the real serum sample, in the presence of 100 pg mL^{-1} pure CKMB using 1:100 $[Ru(bpy)_3]Cl_2$-TPrA solution containing 10 mM PBS, pH 7.4 at 21.5 ± 0.5°C (n=3). First, two bars show 0 pg mL^{-1} CKMB and 100 pg mL^{-1} CKMB in buffer, next 4 bars show results with 100 pg mL^{-1} CKMB spiked in each dilution of serum.

S5. X-ray Diffraction (XRD)

For the XRD characterization, the sample suspension was prepared into thin-film by Doctor Blade method. The XRD measurements were recorded at a scan rate of 5 °/min for 2θ range of 20° to 80° with CuKα radiation of 1.54181 Å.

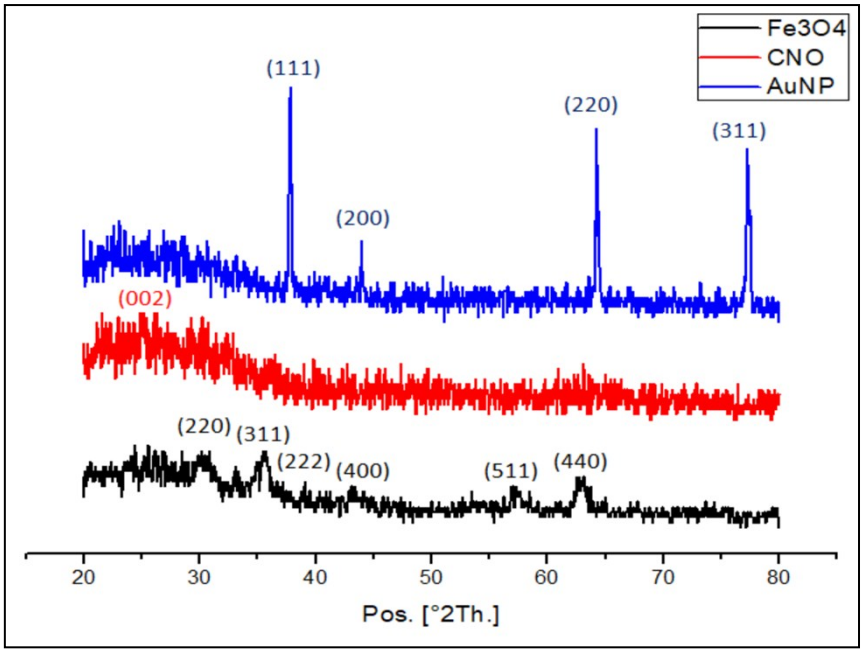

Fig. S10 X-ray diffraction patterns of Fe_3O_4 (black), carbon nano-onion (red) and Au nanoparticles (blue) with their corresponding Bragg reflections.

The XRD pattern of Fe_3O_4 is indexed to the cubic spinel structure with a space group of *Fd-3m* whilst carbon nano onion indicates a peak at 2θ = 25.9° which corresponds to hexagonal structure of graphite[1]. The XRD peaks of Fe_3O_4 and carbon nano onion appeared to be broadened which might be due to Scherrer broadening because of the small particle size of the nanoparticles respectively. The AuNP XRD pattern conforms to the cubic fluorite structure with a space group of *Fm3m.*

Supplementary References:

1 V. Dhand, S. Prasad, M.V. Rao, S. Bharadwaj, Y. Anjaneyulu, and P.K. Jain, *Materials Science and Engineering: C,* 2013, 33(2):758-762.